

ORBGRAND Is Exactly Capacity-achieving via Rank Companding

Zhuang Li and Wenyi Zhang, *Senior Member, IEEE*

Abstract—Among guessing random additive noise decoding (GRAND) algorithms, ordered reliability bits GRAND (ORBGRAND) has attracted considerable attention due to its efficient use of soft information and suitability for hardware implementation. It has also been shown that ORBGRAND achieves a rate very close to the capacity of an additive white Gaussian noise channel under antipodal signaling. In this work, it is further established that, for general binary-input memoryless channels under symmetric input distribution, via suitably companding the ranks in ORBGRAND according to the inverse cumulative distribution function (CDF) of channel reliability, the resulting CDF-ORBGRAND algorithm exactly achieves the mutual information, i.e., the symmetric capacity. This result is then applied to bit-interleaved coded modulation (BICM) systems to handle high-order input constellations. Via considering the effects of mismatched decoding due to both BICM and ORBGRAND, it is shown that CDF-ORBGRAND is capable of achieving the BICM capacity, which was initially derived in the literature by treating BICM as a set of independent parallel channels.

Index Terms—Achievable rate, bit-interleaved coded modulation, capacity-achieving, generalized mutual information, guessing random additive noise decoding, ordered reliability bits.

I. INTRODUCTION

Guessing random additive noise decoding (GRAND) [1], [2] has recently attracted attention as a new paradigm of decoding in emerging communication scenarios. GRAND operates by progressively guessing the error pattern (EP) that the transmitted codeword has experienced through the channel. This approach centering around EPs makes the GRAND paradigm well suited for channel coding in the high-rate high-reliability regime [3].

GRAND was originally proposed for hard-decision channels. This is also reflected by its name: only when the noise is discrete it makes sense to “guess” it. For more general channels, such as additive white Gaussian noise (AWGN) channels, incorporating channel soft information can improve decoding performance [4, Ch. 10], and we need to guess the EP rather than the noise itself. Symbol reliability GRAND (SRGRAND) [5] uses a single-bit reliability indicator to mark whether a channel output symbol is reliable. Soft GRAND (SGRAND) [6] directly exploits the exact log-likelihood ratio (LLR) magnitudes of the channel output to determine the sequence of EPs for guessing, thereby fully leveraging the soft information and achieving maximum-likelihood (ML) decoding. However, the requirement of exact LLR magnitudes in SGRAND necessitates on-the-fly generation of EPs, posing challenges for hardware implementation. Another variant of GRAND, ordered reliability bits GRAND (ORBGRAND) [7]

generates EPs based on the ranking of LLR magnitudes rather than their exact values. This approach enables efficient generation of EPs without depending upon exact LLR magnitudes, and streamlines hardware implementation [8]–[10]. It has also been shown in [11] through an information-theoretic analysis that for AWGN channels under antipodal signaling, the rate achieved by ORBGRAND is very close to the channel mutual information, i.e., the capacity in that setup. There also exist several works that treat GRAND for more general channels such as fading channels [12]–[17].

In this paper, we study a modification of ORBGRAND, which essentially adopts a companding technique to transform the rank of each LLR magnitude according to the inverse cumulative distribution function (CDF) of LLR magnitude. The resulting algorithm is thus termed CDF-ORBGRAND. The value of the shape of the CDF of LLR magnitude has been recognized earlier in [7], and a piecewise linear approximation technique has been utilized therein under the term of “full ORBGRAND”; see also [18], [19]. Via such a companding technique, the decoding metric is rendered asymptotically aligned with the channel law, while still maintaining its amenability to hardware implementation. We analyze the achievable rate of CDF-ORBGRAND for general binary-input memoryless channels under symmetric input distribution, and prove via a random coding argument akin to that in [11] that, CDF-ORBGRAND exactly achieves the mutual information, i.e., the symmetric capacity, without any rate loss. In contrast, for fading channels, ORBGRAND without rank companding may incur a significant rate loss compared to the symmetric capacity; see Fig. 1 in Section III-A.

On the basis of CDF-ORBGRAND for binary-input channels, we proceed to the investigation of bit-interleaved coded modulation (BICM) systems [20], [21]. This investigation is motivated by the prevalence of high-order modulation in modern communication systems, wherein BICM has been a widely used technique. By jointly considering the mismatched decoding effects due to both BICM and ORBGRAND, we derive achievable rates of both CDF-ORBGRAND and ORBGRAND for BICM. Remarkably, we show that CDF-ORBGRAND achieves the BICM capacity, which was initially derived in the literature by treating BICM as a set of independent parallel channels [20], and subsequently established by typicality decoding or by mismatched decoding with appropriately chosen metrics [22]. The BICM capacity-achieving property of CDF-ORBGRAND indicates that the rank companding technique is effective even for handling the heterogeneity among bit channels corresponding to different positions of the labeling of constellation symbols. In contrast, without rank companding, the rate loss of ORBGRAND is evident and becomes more substantial as modulation order increases; see Fig. 4 in Section IV-E.

The authors are with Department of Electronic Engineering and Information Science, University of Science and Technology of China, Hefei, China (wenyizha@ustc.edu.cn). This work was supported in part by the National Natural Science Foundation of China under Grant 62231022.

The remaining part of this paper is organized as follows: Section II introduces the system model, along with GRAND and its variants for general binary-input memoryless channels. Section III proves that CDF-ORBGRAND exactly achieves the symmetric capacity. Section IV considers applying ORBGRAND and CDF-ORBGRAND to a BICM system model, and derives their respective achievable rates, revealing that CDF-ORBGRAND achieves the BICM capacity. Section V concludes this paper. Technical proofs are provided in Appendices.

II. PRELIMINARIES

A. System Model

Our basic channel model is a general binary-input memoryless channel, which, without loss of generality, is of input alphabet $\{+1, -1\}$, with the output probability density function (pdf) denoted by $q^+(y)$ when input $x = +1$, and by $q^-(y)$ when input $x = -1$. Here $q^+(y)$ and $q^-(y)$ are general, without assuming any specific structure like symmetry.

A codebook has length N and rate R nats per channel use, corresponding to $\lceil e^{NR} \rceil$ possible messages. When transmitting message w , the corresponding codeword is denoted by $\underline{x}(w) = [x_1(w), \dots, x_N(w)]$. In this paper we conduct a random coding analysis, and hence assume that the elements of $\underline{x}(w)$ are independent and identically distributed (i.i.d.), uniformly drawn from $\{+1, -1\}$. A message W is uniformly selected from $\{1, \dots, \lceil e^{NR} \rceil\}$ for transmission. Given the channel output vector $\underline{Y} = [Y_1, \dots, Y_N]$, we define the LLRs as

$$T_i = \ln \frac{q^+(Y_i)}{q^-(Y_i)}, \quad i = 1, \dots, N,$$

and call their magnitudes, $[|T_1|, \dots, |T_N|]$, the channel reliability vector. The CDF of $|T|$ is denoted by $\Psi(t)$, for $t \geq 0$. We also introduce the sets $\mathcal{R}_1 = \{y | q^+(y) < q^-(y)\}$ and $\mathcal{R}_2 = \{y | q^+(y) > q^-(y)\}$.

For $i = 1, \dots, N$, we denote R_i as the rank of $|T_i|$ among the channel reliability vector, from 1 (the smallest) to N (the largest).

For our analysis, we impose a few additional assumptions on the behavior of $q^+(y)$ and $q^-(y)$, as follows.

Assumption 1: Both $q^+(y)$ and $q^-(y)$ are light-tailed, in the sense that there exists a sufficiently large constant $M_1 > 0$, a constant $a > 0$ and a polynomial $S_1(\cdot)$ satisfying

$$q^\pm(y) < S_1(|y|)e^{-a|y|}, \quad \forall |y| > M_1. \quad (1)$$

Assumption 2: The growth of $|t| = \left| \ln \frac{q^+(y)}{q^-(y)} \right|$ is polynomially bounded; that is, there exists a sufficiently large constant $M_2 > 0$ and a polynomial $S_2(\cdot)$ satisfying $|t| < S_2(|y|)$, $\forall |y| > M_2$.

Assumption 3: The CDF of $|T|$, $\Psi(\cdot)$, and its inverse, $\Psi^{-1}(\cdot)$, are smooth with finite first, second, and third derivatives.

B. GRAND and Its Variants

Upon receiving a channel output vector y , we compute the channel reliability vector $[|t_1|, \dots, |t_N|]$ and the corresponding hard-decision vector $\underline{x}_{\text{hard}} = [\text{sgn}(t_1), \dots, \text{sgn}(t_N)]$,

where $t_i = \ln \frac{q^+(y_i)}{q^-(y_i)}$ is the LLR and $\text{sgn}(t) = 1$ if $t \geq 0$ and -1 otherwise.

In general, we can collectively denote the EPs used by GRAND as a $2^N \times N$ ± 1 -valued matrix P : in the q -th query, the q -th row of P is used as the EP for testing, such that if $P_{q,i} = -1$ the sign of the i -th entry of $\underline{x}_{\text{hard}}$ is flipped, and otherwise it remains unchanged. If $\underline{x}_{\text{hard}}$ after flipping is a codeword, it is declared as the decoder output. If all rows of P are exhausted without finding a codeword, a decoding failure is declared.

For ORBGRAND, we arrange the rows of P so that the sum reliability of the q -th row, $\sum_{i: P_{q,i}=-1} r_i$, is non-decreasing with q , where r_i is the rank of $|t_i|$ introduced in the previous subsection. Efficient algorithms for generating such P are available (see, e.g., [7], [8]). Since 2^N is typically an exceedingly large quantity, in practice P is usually truncated to its first Q rows, with Q being the maximum number of queries allowed; for our information-theoretic analysis in this paper, however, we do not consider the effect of truncation and hence all EPs of P will be queried in the worst case.

As shown in [11, Sec. II], ORBGRAND and many other variants of GRAND can be represented by the following unified decoding rule, as long as no truncation of P is applied, i.e., $Q = 2^N$:

$$\hat{w} = \arg \min_{w=1, \dots, \lceil e^{NR} \rceil} \frac{1}{N} \sum_{i=1}^N \gamma_i(y) \cdot \mathbf{1}(\text{sgn}(t_i) \cdot x_i(w) < 0). \quad (2)$$

Different choices of $\{\gamma_i\}_{i=1, \dots, N}$ correspond to different choices of P and thus different variants of GRAND:

- When $\gamma_i(y) = 1$, (2) is the original GRAND [1];
- When $\gamma_i(y) = |t_i|$, (2) is SGRAND [6], which is equivalent to ML decoding;
- When $\gamma_i(y) = \frac{r_i}{N}$, (2) is ORBGRAND [7];
- When $\gamma_i(y) = \Psi^{-1}\left(\frac{r_i}{N+1}\right)$, where Ψ^{-1} denotes the inverse function of the CDF of $|T|$, $\Psi^{-1}(2)$ is called CDF-ORBGRAND.

The form of (2) facilitates information-theoretic analysis, as will be conducted in the following sections. A decoding error event occurs if $\hat{W} \neq W$, where \hat{W} is the decoder output, and we define the achievable rate of GRAND as follows.

Definition 1: For the system model in Section II-A, a rate R is achievable under GRAND with given $\{\gamma_i\}_{i=1, \dots, N}$ if there exists a sequence of codebooks of length $N = 1, 2, \dots$, such that the average error probability of decoding for the decoding rule (2) asymptotically vanishes as N grows without bound.

If we do not restrict the decoding rule to be (2) and apply ML decoding, then for our system model in Section II-A, according to Shannon's channel coding theorem, the supremum of all achievable rates is the mutual information $I(X; Y)$ with X uniformly distributed over $\{+1, -1\}$. This mutual information thus serves as the ultimate performance limit for the considered system model, and is termed the symmetric capacity in the sequel.

¹In statistics, Ψ^{-1} is also called the quantile function of $|T|$.

III. CAPACITY-ACHIEVING PROPERTY OF CDF-ORBGRAND

To motivate CDF-ORBGRAND, it is helpful to inspect the decoding rule (2). Based on the convergence of empirical distributions, as N gets large, with high probability, $R_i/(N+1)$ gets close to $\Psi(|T_i|)$.² Thus, by conducting the inverse operation, i.e., Ψ^{-1} , over $R_i/(N+1)$, we essentially return to $|T_i|$, and this is exactly what CDF-ORBGRAND does. Due to this intuitive argument, CDF-ORBGRAND should behave similarly to SGRAND asymptotically, and this assertion will be formalized and established in this section. Since $\{\gamma_i\}_{i=1,\dots,N}$ simply compands the ranks $\{R_i\}_{i=1,\dots,N}$, the corresponding EP queries can also be generated in a similar fashion to those of ORBGRAND.

A. Main Result

Neither ORBGRAND nor CDF-ORBGRAND is ML decoding, and furthermore, their metrics, $\{\gamma_i\}_{i=1,\dots,N}$, are N correlated random variables due to ranking. Therefore, we cannot directly invoke existing information-theoretic formulas for evaluating their achievable rates. In this paper, we essentially establish the achievable rate of CDF-ORBGRAND as the generalized mutual information (GMI) of the considered decoding rule, following the general approach of mismatched decoding (see, e.g., [23], [24]). As revealed by the result below, although CDF-ORBGRAND is inherently mismatched, its achievable rate exactly coincides with the symmetric capacity. In other words, from an information-theoretic perspective, no rate loss is incurred when applying CDF-ORBGRAND.

Theorem 1: For the system model in Section II-A, CDF-ORBGRAND achieves the symmetric capacity, i.e.,

$$I(X; Y) = \ln 2 - \frac{1}{2} \int_{-\infty}^{\infty} \ln \left(1 + \frac{q^-(y)}{q^+(y)} \right) q^+(y) dy - \frac{1}{2} \int_{-\infty}^{\infty} \ln \left(1 + \frac{q^+(y)}{q^-(y)} \right) q^-(y) dy \quad (3)$$

in nats/channel use.

Proof: See Section III-B. ■

In our previous work [25], we have derived the GMI of ORBGRAND for the system model in Section II-A as

$$I_{\text{ORB}} = \ln 2 - \inf_{\theta < 0} \left\{ \int_0^1 \ln(1 + e^{\theta t}) dt - \theta \cdot \frac{1}{2} \int_{\mathcal{R}_1} \Psi \left(\left| \ln \frac{q^+(y)}{q^-(y)} \right| \right) q^+(y) dy - \theta \cdot \frac{1}{2} \int_{\mathcal{R}_2} \Psi \left(\left| \ln \frac{q^+(y)}{q^-(y)} \right| \right) q^-(y) dy \right\} \quad (4)$$

²This observation has been used in [11] to explain the behavior of ORBGRAND, by introducing a variant of GRAND termed cdf-GRAND therein. Unfortunately, cdf-GRAND relies on the exact channel reliability vector, and hence is still not amenable to hardware implementation.

in nats/channel use. According to the proof of Theorem 1 in Section III-B, the symmetric capacity (3) can be equivalently rewritten as

$$I_{\text{CDF-ORB}} = \ln 2 - \inf_{\theta < 0} \left\{ \mathbb{E} \left[\ln \left(1 + e^{\theta \cdot \left| \ln \frac{q^+(Y)}{q^-(Y)} \right|} \right) \right] - \theta \cdot \frac{1}{2} \int_{\mathcal{R}_1} \left| \ln \frac{q^+(y)}{q^-(y)} \right| q^+(y) dy - \theta \cdot \frac{1}{2} \int_{\mathcal{R}_2} \left| \ln \frac{q^+(y)}{q^-(y)} \right| q^-(y) dy \right\} \quad (5)$$

in nats/channel use. Comparing (4) and (5), we observe that their difference lies in that for CDF-ORBGRAND the integrands are $\left| \ln \frac{q^+(y)}{q^-(y)} \right|$ and for ORBGRAND the corresponding integrands are replaced by $\Psi \left(\left| \ln \frac{q^+(y)}{q^-(y)} \right| \right)$.³

We conduct some numerical experiments to compare (4) and (5), for antipodal signaling, i.e., BPSK modulation, over AWGN, additive white Laplacian noise (AWLN), and Rayleigh fading channels with receiver-side perfect channel state information (CSI). These channels can be written as

$$Y = \sqrt{P}HX + Z$$

- AWGN channel, $H = 1$ and $Z \sim \mathcal{N}(0, 1)$: $T = 2\sqrt{P}Y$.
- AWLN channel, $H = 1$ and $Z \sim \text{Laplace}(0, \frac{1}{\sqrt{2}})$: $T = \sqrt{2}(|Y + \sqrt{P}| - |Y - \sqrt{P}|)$.
- Rayleigh fading channel with receiver-side perfect CSI, $H \sim \mathcal{CN}(0, 1)$ and $Z \sim \mathcal{CN}(0, 1)$: $T = 4\sqrt{P}\Re(H^*Y)$. We point out that here $q^\pm(\cdot)$ should be evaluated for the augmented channel output (y, h) , i.e., including the receiver-side perfect CSI.⁴

The curves of I_{ORB} and $I_{\text{CDF-ORB}}$ for different signal-to-noise ratio (SNR) values are displayed in Fig. 1. Their comparison indicates that in AWGN channel, ORBGRAND almost achieves the symmetric capacity, a result already established in [11]; that in AWLN channel, a noticeable gap appears; and that for Rayleigh fading channel, the gap becomes even more pronounced.

B. Proof of Main Result

Based on the unified decoding rule (2), the decoding metric of CDF-ORBGRAND is given by

$$D(w) = \frac{1}{N} \sum_{i=1}^N \Psi^{-1} \left(\frac{R_i}{N+1} \right) \cdot \mathbf{1}(\text{sgn}(T_i) \cdot X_i(w) < 0), \quad (6)$$

for $w = 1, \dots, \lceil e^{NR} \rceil$.

Since the terms in the summation in (6) involve ranks of channel reliabilities, they are correlated, and hence the

³It can be readily shown that with this replacement the first expectation term in the bracket of (5) becomes the integral $\int_0^1 \ln(1 + e^{\theta t}) dt$ of (4), since $\Psi(|T|)$ is a uniform random variable over the unit interval.

⁴We clarify that in the numerical experiments in [25], the GMI of ORBGRAND for this setup was incorrectly computed, due to an error in the program evaluating the integrals in (4). In the current paper, we rectify the error and provide updated numerical results. The program code can be found at: <https://github.com/ustclizhuang/Simulation>

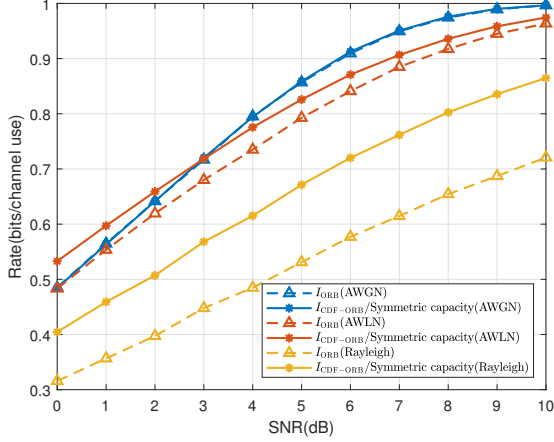


Fig. 1. Comparison between I_{ORB} and $I_{\text{CDF-ORB}}$ under AWGN, AWLN, and Rayleigh fading channels. Since Rayleigh fading channels are described in complex baseband, the SNR is defined as the effective per-dimension SNR, corresponding to the in-phase component of the received signal.

standard GMI formula (see, e.g., [23, Eqn. (12)]) cannot be straightforwardly applied. Therefore we conduct the analysis directly from the first principle, akin to that in [11], [25] and dating back to [24], [26]. We calculate the ensemble average error probability of decoding, which, for the i.i.d. random coding ensemble in our system model, is equivalent to the error probability of decoding when message $w = 1$ is transmitted.

Under the condition that the transmitted message is $w = 1$, some asymptotic properties of the CDF-ORBGRAND decoding metric (6) are presented in the following lemmas, whose proofs are provided in the appendices.

Lemma 1: As $N \rightarrow \infty$, the expectation of the decoding metric (6) for the transmitted codeword $w = 1$ is given by

$$\lim_{N \rightarrow \infty} \mathbb{E}D(1) = \frac{1}{2} \int_{\mathcal{R}_1} \left| \ln \frac{q^+(y)}{q^-(y)} \right| q^+(y) dy + \frac{1}{2} \int_{\mathcal{R}_2} \left| \ln \frac{q^+(y)}{q^-(y)} \right| q^-(y) dy. \quad (7)$$

Lemma 2: As $N \rightarrow \infty$, the variance of the decoding metric (6) for the transmitted codeword $w = 1$ satisfies

$$\lim_{N \rightarrow \infty} \text{var}D(1) = 0. \quad (8)$$

Lemma 3: As $N \rightarrow \infty$, for any non-transmitted codeword, i.e., $w' \neq 1$, and for any $\theta < 0$, the decoding metric (6) behaves almost surely as

$$\lim_{N \rightarrow \infty} \frac{1}{N} \ln \mathbb{E} \left\{ e^{N\theta D(w')} \middle| \underline{\mathbb{I}} \right\} = \mathbb{E} \left[\ln \left(1 + e^{\theta \cdot \left| \ln \frac{q^+(y)}{q^-(y)} \right|} \right) \right] - \ln 2. \quad (9)$$

With these lemmas, we proceed to prove Theorem 1.

For any $\epsilon > 0$, define the event \mathcal{U}_ϵ as

$$\mathcal{U}_\epsilon = \left\{ D(1) \geq \frac{1}{2} \int_{\mathcal{R}_1} \left| \ln \frac{q^+(y)}{q^-(y)} \right| q^+(y) dy + \frac{1}{2} \int_{\mathcal{R}_2} \left| \ln \frac{q^+(y)}{q^-(y)} \right| q^-(y) dy + \epsilon \right\},$$

corresponding to the case where the decoding metric of the transmitted message, $D(1)$, exceeds its expectation (Lemma 1) by at least ϵ . Consequently, the ensemble average error probability of decoding can be expressed as

$$\begin{aligned} & \Pr[\hat{W} \neq 1] \\ &= \Pr[\hat{W} \neq 1 | \mathcal{U}_\epsilon] \Pr[\mathcal{U}_\epsilon] + \Pr[\hat{W} \neq 1, \mathcal{U}_\epsilon^c] \\ &\leq \Pr[\mathcal{U}_\epsilon] + \Pr[\hat{W} \neq 1, \mathcal{U}_\epsilon^c]. \end{aligned} \quad (10)$$

Using Lemmas 1 and 2, along with Chebyshev inequality, we obtain that for any $\epsilon > 0$,

$$\lim_{N \rightarrow \infty} \Pr \left[D(1) \geq \frac{1}{2} \int_{\mathcal{R}_1} \left| \ln \frac{q^+(y)}{q^-(y)} \right| q^+(y) dy + \frac{1}{2} \int_{\mathcal{R}_2} \left| \ln \frac{q^+(y)}{q^-(y)} \right| q^-(y) dy + \epsilon \right] = 0. \quad (11)$$

Therefore, $\Pr[\mathcal{U}_\epsilon]$ can be made arbitrarily small as N tends to infinity.

On the other hand, from the decoding rule (2) together with the union bound, we obtain

$$\begin{aligned} & \Pr[\hat{W} \neq 1, \mathcal{U}_\epsilon^c] \\ &\leq \Pr \left[\exists w' \neq 1, D(w') < \frac{1}{2} \int_{\mathcal{R}_1} \left| \ln \frac{q^+(y)}{q^-(y)} \right| q^+(y) dy + \frac{1}{2} \int_{\mathcal{R}_2} \left| \ln \frac{q^+(y)}{q^-(y)} \right| q^-(y) dy + \epsilon \right] \\ &\leq e^{NR} \Pr \left[D(w') < \frac{1}{2} \int_{\mathcal{R}_1} \left| \ln \frac{q^+(y)}{q^-(y)} \right| q^+(y) dy + \frac{1}{2} \int_{\mathcal{R}_2} \left| \ln \frac{q^+(y)}{q^-(y)} \right| q^-(y) dy + \epsilon \right]. \end{aligned} \quad (12)$$

Considering the probability in (12) conditioned upon $\underline{\mathbb{I}}$, and applying Chernoff bound, we obtain that for any N and any $\theta < 0$,

$$\begin{aligned} & -\frac{1}{N} \ln \Pr \left[D(w') < \frac{1}{2} \int_{\mathcal{R}_1} \left| \ln \frac{q^+(y)}{q^-(y)} \right| q^+(y) dy + \frac{1}{2} \int_{\mathcal{R}_2} \left| \ln \frac{q^+(y)}{q^-(y)} \right| q^-(y) dy + \epsilon \middle| \underline{\mathbb{I}} \right] \\ &\geq \theta \cdot \left[\frac{1}{2} \int_{\mathcal{R}_1} \left| \ln \frac{q^+(y)}{q^-(y)} \right| q^+(y) dy + \frac{1}{2} \int_{\mathcal{R}_2} \left| \ln \frac{q^+(y)}{q^-(y)} \right| q^-(y) dy + \epsilon \right] - \frac{1}{N} \ln \mathbb{E} \left\{ e^{N\theta D(w')} \middle| \underline{\mathbb{I}} \right\}. \end{aligned} \quad (13)$$

Letting $\epsilon \rightarrow 0, N \rightarrow \infty$, and applying the almost sure limit in Lemma 3, we obtain

$$\begin{aligned} & \Pr \left[D(w') < \frac{1}{2} \int_{\mathcal{R}_1} \left| \ln \frac{q^+(y)}{q^-(y)} \right| q^+(y) dy \right. \\ & \quad \left. + \frac{1}{2} \int_{\mathcal{R}_2} \left| \ln \frac{q^+(y)}{q^-(y)} \right| q^-(y) dy + \epsilon \left\lfloor \frac{\mathbb{T}}{\epsilon} \right\rfloor \right] \\ & \leq \exp \left\{ -N \left[\ln 2 - \mathbb{E} \left[\ln \left(1 + e^{\theta \cdot \left| \ln \frac{q^+(Y)}{q^-(Y)} \right|} \right) \right] \right. \right. \\ & \quad \left. \left. + \theta \cdot \frac{1}{2} \int_{\mathcal{R}_1} \left| \ln \frac{q^+(y)}{q^-(y)} \right| q^+(y) dy \right. \right. \\ & \quad \left. \left. + \theta \cdot \frac{1}{2} \int_{\mathcal{R}_2} \left| \ln \frac{q^+(y)}{q^-(y)} \right| q^-(y) dy \right] \right\}. \quad (14) \end{aligned}$$

Then applying the law of total expectation to remove the conditioning in the left side of (14) and substituting the right side upper bound into (12), we establish that the ensemble average error probability of decoding vanishes asymptotically as $N \rightarrow \infty$, whenever the rate R satisfies

$$\begin{aligned} R < I_{\text{CDF-ORB}} := \ln 2 - \inf_{\theta < 0} \left\{ \mathbb{E} \left[\ln \left(1 + e^{\theta \cdot \left| \ln \frac{q^+(Y)}{q^-(Y)} \right|} \right) \right] \right. \\ & \quad \left. - \theta \cdot \frac{1}{2} \int_{\mathcal{R}_1} \left| \ln \frac{q^+(y)}{q^-(y)} \right| q^+(y) dy \right. \\ & \quad \left. - \theta \cdot \frac{1}{2} \int_{\mathcal{R}_2} \left| \ln \frac{q^+(y)}{q^-(y)} \right| q^-(y) dy \right\}. \quad (15) \end{aligned}$$

Now we prove that $I_{\text{CDF-ORB}}$ is equivalent to the mutual information $I(\mathbf{X}; \mathbf{Y})$, i.e., symmetric capacity. By noting that $\left| \ln \frac{q^+(y)}{q^-(y)} \right| = \ln \frac{q^-(y)}{q^+(y)}$ for $y \in \mathcal{R}_1$ and $\left| \ln \frac{q^+(y)}{q^-(y)} \right| = \ln \frac{q^+(y)}{q^-(y)}$ for $y \in \mathcal{R}_2$, we can rewrite the mutual information (3) as

$$\begin{aligned} I(\mathbf{X}; \mathbf{Y}) &= \ln 2 - \frac{1}{2} \int_{\mathcal{R}_1} \ln \left(1 + e^{\left| \ln \frac{q^+(y)}{q^-(y)} \right|} \right) q^+(y) dy \\ & \quad - \frac{1}{2} \int_{\mathcal{R}_2} \ln \left(1 + e^{-\left| \ln \frac{q^+(y)}{q^-(y)} \right|} \right) q^+(y) dy \\ & \quad - \frac{1}{2} \int_{\mathcal{R}_1} \ln \left(1 + e^{-\left| \ln \frac{q^+(y)}{q^-(y)} \right|} \right) q^-(y) dy \\ & \quad - \frac{1}{2} \int_{\mathcal{R}_2} \ln \left(1 + e^{\left| \ln \frac{q^+(y)}{q^-(y)} \right|} \right) q^-(y) dy. \quad (16) \end{aligned}$$

By using the fact that $q(y) = \frac{1}{2}(q^+(y) + q^-(y))$, we can further rewrite (16) as

$$\begin{aligned} I(\mathbf{X}; \mathbf{Y}) &= \ln 2 - \mathbb{E} \left[\ln \left(1 + e^{-\left| \ln \frac{q^+(Y)}{q^-(Y)} \right|} \right) \right] \\ & \quad - \frac{1}{2} \int_{\mathcal{R}_1} \left| \ln \frac{q^+(y)}{q^-(y)} \right| q^+(y) dy - \frac{1}{2} \int_{\mathcal{R}_2} \left| \ln \frac{q^+(y)}{q^-(y)} \right| q^-(y) dy. \quad (17) \end{aligned}$$

On the other hand, consider the right side of (15) as a function of $\theta < 0$:

$$\begin{aligned} I_{\text{CDF-ORB}} &= \sup_{\theta < 0} f(\theta), \quad (18) \\ f(\theta) &:= \ln 2 - \mathbb{E} \left[\ln \left(1 + e^{\theta \cdot \left| \ln \frac{q^+(Y)}{q^-(Y)} \right|} \right) \right] \\ & \quad + \frac{\theta}{2} \int_{\mathcal{R}_1} \left| \ln \frac{q^+(y)}{q^-(y)} \right| q^+(y) dy + \frac{\theta}{2} \int_{\mathcal{R}_2} \left| \ln \frac{q^+(y)}{q^-(y)} \right| q^-(y) dy. \quad (19) \end{aligned}$$

Therefore, we obtain the following inequalities:

$$I(\mathbf{X}; \mathbf{Y}) \geq I_{\text{CDF-ORB}} \geq f(-1) = I(\mathbf{X}; \mathbf{Y}), \quad (20)$$

implying that $I_{\text{CDF-ORB}} = I(\mathbf{X}; \mathbf{Y})$, and that $f(\theta)$ attains its maximum at $\theta = -1$. This completes the proof.

IV. APPLICATION OF CDF-ORBGRAND IN BICM

High-order modulation has been a prevailing technique in contemporary communication systems, for achieving high spectral efficiency. In order to apply GRAND to high-order modulation, we study BICM systems, where a high-order coded modulation is effectively decomposed into multiple bit channels, with the decoding metric for each bit channel separately computed. Remarkably, we establish that CDF-ORBGRAND is capable of achieving the BICM capacity, which was initially derived in the literature by treating the decomposed bit channels as independent.

A. BICM System Model

BICM employs an encoder, a bit interleaver π , and a binary labeling function $\mu : \{+1, -1\}^m \rightarrow \mathcal{S}$ that maps blocks of m bits to symbols in a constellation \mathcal{S} . Let us start with a codebook of length mN and rate R nats per channel use, containing $\lceil e^{NR} \rceil$ codewords. When message w is selected for transmission, the corresponding codeword is denoted by $\tilde{\mathbf{x}}(w)$. The codeword is then passed through the interleaver, and the resulting interleaved codeword is denoted by

$$\begin{aligned} \underline{\mathbf{x}}(w) &= \pi(\tilde{\mathbf{x}}(w)) \\ &= [x_{1,1}(w), \dots, x_{1,m}(w), \dots, x_{N,1}(w), \dots, x_{N,m}(w)]. \end{aligned}$$

For notational convenience, in the sequel, $\underline{\mathbf{x}}(w)$ will be referred to as the codeword, and the original codeword $\tilde{\mathbf{x}}(w)$, which can be recovered from $\underline{\mathbf{x}}(w)$ through a de-interleaving operation, will not be needed in the analysis. Since we consider random coding, elements of $\underline{\mathbf{x}}(w)$ are i.i.d., uniformly drawn from $\{+1, -1\}$. After modulation, the m bits $x_{i,1}(w), \dots, x_{i,m}(w)$ as a block are mapped via the binary labeling function μ into a symbol $s_i(w)$, and the transmitted symbol sequence is denoted by

$$\underline{s}(w) = [s_1(w), \dots, s_N(w)].$$

The elements of the codeword corresponding to the j -th bit of the labeling are denoted by

$$\underline{x}_j(w) = [x_{1,j}(w), \dots, x_{N,j}(w)],$$

for $j = 1, \dots, m$. Conversely, we define the inverse mapping of the j -th bit of the labeling as $b_j : \mathcal{S} \rightarrow \{+1, -1\}$; that is,

$b_j(s)$ is the codeword bit corresponding to the j -th position of the transmitted symbol s . The received sequence is denoted by $\underline{Y} = [Y_1, \dots, Y_N]$.

We consider a general memoryless channel, where the output pdf of Y_i under input bit $x_{i,j} = +1$ is denoted by $q_j^+(y)$, and under input bit $x_{i,j} = -1$ is denoted by $q_j^-(y)$, respectively. These pdfs can be evaluated as

$$q_j^+(y) = \frac{1}{|\mathcal{S}_j^+|} \sum_{s \in \mathcal{S}_j^+} p(y|s), \quad q_j^-(y) = \frac{1}{|\mathcal{S}_j^-|} \sum_{s \in \mathcal{S}_j^-} p(y|s),$$

where \mathcal{S}_j^+ and \mathcal{S}_j^- denote the sets of constellation symbols whose j -th bit equals $+1$ and -1 , respectively. For each $j = 1, \dots, m$, we also assume that $q_j^+(y)$ and $q_j^-(y)$ satisfy Assumptions 1, 2 and 3 introduced in Section II-A.

Define the LLR $T_{i,j} = \ln \frac{q_j^+(Y_i)}{q_j^-(Y_i)}$ and the reliability vector

$$[|T_{1,1}|, \dots, |T_{1,m}|, \dots, |T_{N,1}|, \dots, |T_{N,m}|].$$

For $i = 1, \dots, N$ and $j = 1, \dots, m$, denote by $R_{i,j}$ the rank of $|T_{i,j}|$ among the sorted array consisting of $\{|T_{1,1}|, \dots, |T_{1,m}|, \dots, |T_{N,1}|, \dots, |T_{N,m}|\}$, from 1 (the smallest) to mN (the largest). Let $\Psi_1(t), \dots, \Psi_m(t)$ be the CDFs of $|T_{\cdot,1}|, \dots, |T_{\cdot,m}|$ for $t \geq 0$, respectively. We further define the average CDF as

$$\bar{\Psi}(t) = \frac{1}{m} \sum_{j=1}^m \Psi_j(t). \quad (21)$$

We also introduce the sets $\mathcal{R}_{1,j} = \{y | q_j^+(y) < q_j^-(y)\}$ and $\mathcal{R}_{2,j} = \{y | q_j^+(y) > q_j^-(y)\}$.

B. BICM Capacity

Analysis of BICM was initially conducted under the assumption of ideal interleaving [20], treating the BICM system model as m mutually independent parallel binary-input memoryless channels, the j -th one corresponding to the j -th bit of the labeling of the constellation symbols, with output pdf $q_j^+(y)$ under input $x = +1$ and $q_j^-(y)$ under input $x = -1$; see Fig. 2 for an illustration.

Based on this parallel channel model, the BICM system achieves the rate, i.e., the BICM capacity,

$$C^{\text{BICM}} = \sum_{j=1}^m I(X_j; Y), \quad (22)$$

where in the j -th term of the summation, X_j is uniformly distributed over $\{+1, -1\}$, and Y is driven by $q_j^\pm(y)$, as described in the previous paragraph.

Treating the m bits within a symbol as independent is in fact a mismatched decoding rule, which can be expressed as [21], [27]

$$\hat{w} = \arg \max_{w=1, \dots, \lceil e^{NR} \rceil} \prod_{i=1}^N \prod_{j=1}^m d_j(b_j(s_i(w)), y_i), \quad (23)$$

where the j -th bit decoding metric is

$$d_j(b_j(s) = +1, y) = q_j^+(y), \quad d_j(b_j(s) = -1, y) = q_j^-(y).$$

Via leveraging the tool of mismatched decoding, it has been shown that the BICM decoding rule (23) achieves the BICM capacity (22) even in the absence of ideal interleaving [22].

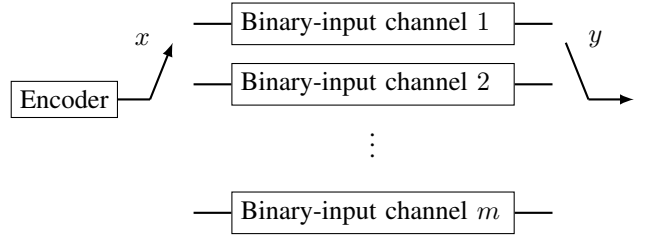


Fig. 2. Parallel channel model of BICM with ideal interleaving.

C. GRAND and Its Variants for BICM

After receiving a channel output vector \underline{y} , we compute the channel reliability vector

$$[|t_{1,1}|, \dots, |t_{1,m}|, \dots, |t_{N,1}|, \dots, |t_{N,m}|]$$

and the corresponding hard-decision vector

$$\underline{x}_{\text{hard}} = [\kappa_{1,1}, \dots, \kappa_{1,m}, \dots, \kappa_{N,1}, \dots, \kappa_{N,m}],$$

where $t_{i,j} = \ln \frac{q_j^+(y_i)}{q_j^-(y_i)}$ is the LLR and $\kappa_{i,j} = \text{sgn}(t_{i,j})$.

GRAND algorithms for BICM have a $2^{mN} \times mN$ ± 1 -valued matrix P for representing EPs, wherein the q -th row is denoted as

$$P_q = [P_{q,1,1}, \dots, P_{q,1,m}, \dots, P_{q,N,1}, \dots, P_{q,N,m}],$$

for conducting the q -th query: if $P_{q,i,j} = -1$, the sign of $\kappa_{i,j}$ in $\underline{x}_{\text{hard}}$ is flipped, and otherwise it remains unchanged. If $\underline{x}_{\text{hard}}$ after flipping is a codeword, it is declared as the decoder output. If all rows of P are exhausted without finding a codeword, a decoding failure is declared. For ORBGRAND, we arrange the rows of P so that the sum reliability of the q -th row, $\sum_{i,j:P_{q,i,j}=-1} r_{i,j}$, is non-decreasing with q , where $r_{i,j}$ is the rank of $|t_{i,j}|$.

Similar to Section II-B, we have the following unified decoding rule for GRAND algorithms:

$$\hat{w} = \arg \min_{w=1, \dots, \lceil e^{NR} \rceil} \frac{1}{mN} \sum_{i=1}^N \sum_{j=1}^m \gamma_{i,j}(y) \cdot \mathbf{1}(\kappa_{i,j} x_{i,j}(w) < 0), \quad (24)$$

for which different choices of $\gamma_{i,j}$ correspond to different variants of GRAND under BICM:

- When $\gamma_{i,j}(y) = 1$, (24) is the original GRAND;
- When $\gamma_{i,j}(y) = |t_{i,j}|$, (24) is SGRAND, and is equivalent to the decoding rule in (23); see Appendix D for a proof of their equivalence;
- When $\gamma_{i,j}(y) = \frac{r_{i,j}}{mN}$, (24) is ORBGRAND;
- When $\gamma_{i,j}(y) = \bar{\Psi}^{-1}\left(\frac{r_{i,j}}{mN+1}\right)$, where $\bar{\Psi}^{-1}$ denotes the inverse function of $\bar{\Psi}$ given by (21), (24) is CDF-ORBGRAND.

D. Rate Analysis

The following theorem establishes that CDF-ORBGRAND achieves the BICM capacity.

Theorem 2: For the system model in Section IV-A, CDF-ORBGRAND achieves the BICM capacity, i.e.,

$$I_{\text{CDF-ORB,BICM}} = C^{\text{BICM}}. \quad (25)$$

Proof: See Appendix E. ■

For comparison, the following theorem provides the achievable rate of ORBGRAND for BICM.

Theorem 3: For the system model in Section IV-A, ORBGRAND achieves the GMI

$$I_{\text{ORB,BICM}} = m \ln 2 - \inf_{\theta < 0} \left\{ \sum_{j=1}^m \left(\int_0^1 \ln(1 + e^{\theta t}) dt \right. \right. \\ \left. \left. - \frac{\theta}{2} \int_{\mathcal{R}_{1,j}} \bar{\Psi} \left(\left| \ln \frac{q_j^+(y)}{q_j^-(y)} \right| \right) q_j^+(y) dy \right. \right. \\ \left. \left. - \frac{\theta}{2} \int_{\mathcal{R}_{2,j}} \bar{\Psi} \left(\left| \ln \frac{q_j^+(y)}{q_j^-(y)} \right| \right) q_j^-(y) dy \right) \right\} \quad (26)$$

in nats/channel use.

Proof: See Appendix E. ■

E. Numerical Results

In this subsection, we numerically evaluate $I_{\text{CDF-ORB,BICM}}$ and $I_{\text{ORB,BICM}}$ for QPSK, 8PSK, and 16QAM, over Rayleigh fading channel with receiver-side perfect CSI. For each constellation, we consider both Gray and set-partitioning (SP) labeling schemes. As an illustration, Fig. 3 presents the 16QAM constellation diagrams corresponding to Gray and SP labelings. The channel input–output relationship is given by

$$Y = HS + Z,$$

where $H \sim \mathcal{CN}(0, 1)$ is the channel fading coefficient, S is the channel input corresponding to a constellation symbol, and $Z \sim \mathcal{CN}(0, 1)$ is the AWGN. The average SNR is thus $\mathbb{E}[|S|^2]$.

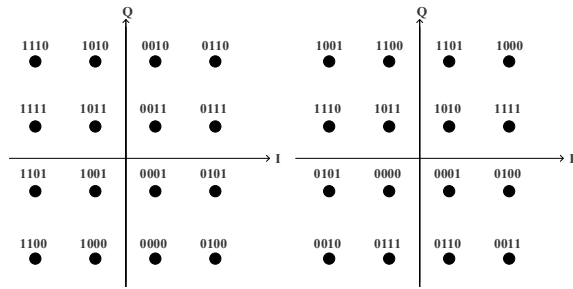


Fig. 3. Gray (left) and SP (right) labelings for 16QAM. Here 0 and 1 correspond to -1 and $+1$, respectively.

The numerical results are shown in Fig. 4. It can be observed that ORBGRAND incurs a significant gap to the BICM capacity under both Gray and SP labelings. For example, with 8PSK and Gray labeling at SNR 15 dB, $I_{\text{ORB,BICM}}$ falls short of the BICM capacity (i.e., $I_{\text{CDF-ORB,BICM}}$) by approximately 0.5 bits per channel use. Moreover, this gap grows as the modulation order increases, reflecting the heightened sensitivity of ORBGRAND to high-order modulation in fading channels. Under the same conditions, the gap with SP labeling is slightly

more pronounced than that with Gray labeling, indicating the impact of the choice of labeling scheme.

The performance gain of CDF-ORBGRAND over ORBGRAND can be attributed to the improved alignment of decoding metrics via rank companding, as commented at the beginning of Section III. This phenomenon appears to be the most evident in the intermediate regime of SNR, and as modulation order increases.

In Fig. 4 we also include the achievable rates $\tilde{I}_{\text{ORB,BICM}}$ of BICM derived in [25] which was derived under the assumption of ideal interleaving;⁵ see the end of Appendix E for details. Although the derivation relies upon an ideal assumption, we observe that the curves of $\tilde{I}_{\text{ORB,BICM}}$ are very close to the exact ones of $I_{\text{ORB,BICM}}$, indicating that the ideal interleaving assumption is usually sufficient for practical purposes.

V. CONCLUSION

In this work, we first analyze the achievable rates of ORBGRAND and its variant under rank companding, CDF-ORBGRAND, from the perspective of the GMI for general binary-input memoryless channels. A somewhat unexpected yet basic finding is that the achievable rate of CDF-ORBGRAND is identical to the symmetric capacity, indicating that rank companding loses no information asymptotically. Building upon this finding, we extend the analysis to BICM and demonstrate that, CDF-ORBGRAND also achieves the BICM capacity. By contrast, ORBGRAND sometimes experiences a substantial rate loss in fading channels.

We emphasize that our analytical findings are information-theoretic in nature, which become effective as code lengths grow large. In practical scenarios with finite code lengths, CDF-ORBGRAND still exhibits a performance gap relative to ML decoding. Meanwhile, various practical optimization techniques for ORBGRAND have been proposed to enhance its performance in realistic settings; see, e.g., [7], [8], [11], [18], [19]. In consideration of these, evaluating CDF-ORBGRAND under finite code lengths will be the focus of our future work.

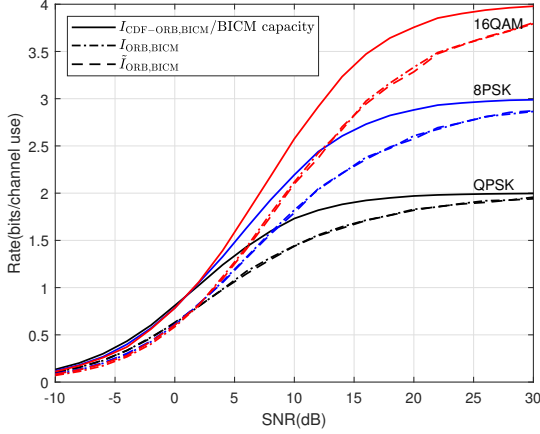
APPENDIX A PROOFS OF LEMMAS 1, 4, AND 7

These three lemmas characterize the asymptotic behavior of the expectation of the decoding metric under $w = 1$ as $N \rightarrow \infty$. We only provide the proof of Lemma 1. Lemmas 4 and 7 appear in the proofs of Theorems 2 and 3, respectively, in Appendix E. Their proofs are similar to that of Lemma 1 and are hence omitted.

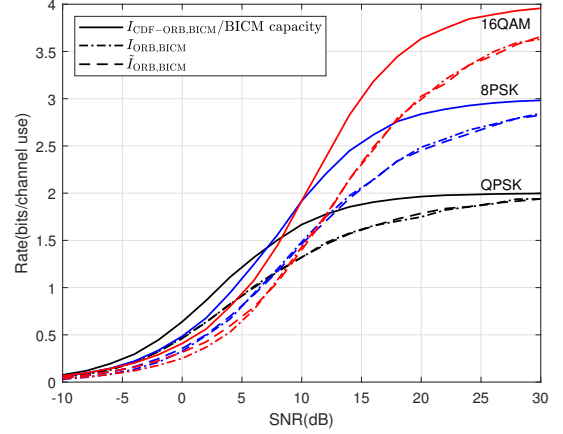
For the decoding metric (6) of CDF-ORBGRAND, we have

$$\mathbb{E}[D(1)] = \frac{1}{N} \sum_{i=1}^N \mathbb{E} \left[\Psi^{-1} \left(\frac{R_i}{N+1} \right) \cdot \mathbf{1}(\text{sgn}(T_i) \cdot X_i(1) < 0) \right]. \quad (27)$$

⁵Similar to Fig. 1, here we rectify an error in the numerical program in [25] and update the numerical results.



(a) Gray labeling



(b) Set-partitioning labeling

Fig. 4. Achievable rates of ORBGRAND, CDF-ORBGRAND, and BICM capacity for QPSK, 8PSK, and 16QAM over Rayleigh fading channel with perfect CSI. Line styles indicate curve type: solid for CDF-ORBGRAND and BICM capacity, dash-dot for ORBGRAND (26), and dashed for ORBGRAND under the assumption of ideal interleaving (64) in [25]. Line colors indicate modulation format: black for QPSK, blue for 8PSK, red for 16QAM.

For each summand in (27), we have

$$\begin{aligned} & \mathbb{E} \left[\Psi^{-1} \left(\frac{R_i}{N+1} \right) \cdot \mathbf{1}(\text{sgn}(T_i) \cdot X_i(1) < 0) \right] \\ &= \frac{1}{2} \mathbb{E} \left[\Psi^{-1} \left(\frac{R_i}{N+1} \right) \cdot \mathbf{1}(T_i < 0) \middle| X_i(1) = +1 \right] \\ & \quad + \frac{1}{2} \mathbb{E} \left[\Psi^{-1} \left(\frac{R_i}{N+1} \right) \cdot \mathbf{1}(T_i > 0) \middle| X_i(1) = -1 \right]. \end{aligned} \quad (28)$$

Considering the first term in (28) and applying the law of total expectation, we obtain

$$\begin{aligned} & \mathbb{E} \left[\Psi^{-1} \left(\frac{R_i}{N+1} \right) \cdot \mathbf{1}(T_i < 0) \middle| X_i(1) = +1 \right] \\ &= \mathbb{E} \left[\mathbb{E} \left[\Psi^{-1} \left(\frac{R_i}{N+1} \right) \cdot \mathbf{1}(T_i < 0) \middle| X_i(1) = +1, Y_i \right] \right], \end{aligned} \quad (29)$$

for which

$$\begin{aligned} & \mathbb{E} \left[\Psi^{-1} \left(\frac{R_i}{N+1} \right) \cdot \mathbf{1}(T_i < 0) \middle| X_i(1) = +1, Y_i = y \right] \\ &= \mathbb{E} \left[\Psi^{-1} \left(\frac{R_i}{N+1} \right) \cdot \mathbf{1}(q^+(y) < q^-(y)) \middle| X_i(1) = +1, Y_i = y \right] \\ &= \begin{cases} \mathbb{E} \left[\Psi^{-1} \left(\frac{R_i}{N+1} \right) \middle| X_i(1) = +1, Y_i = y \right] & \text{if } q^+(y) < q^-(y), \\ 0 & \text{else.} \end{cases} \end{aligned} \quad (30)$$

Note that R_i in (30) is the rank of $|t| = \left| \ln \frac{q^+(y)}{q^-(y)} \right|$ when inserted into a sorted array of $N-1$ i.i.d. samples of $|T|$, and

we denote by $u(y)$ the upper branch of (30). Hence we have

$$\begin{aligned} & \mathbb{E} \left[\Psi^{-1} \left(\frac{R_i}{N+1} \right) \cdot \mathbf{1}(T_i < 0) \middle| X_i(1) = +1 \right] \\ &= \int_{\mathcal{R}_1} u(y) q^+(y) dy. \end{aligned} \quad (31)$$

Similarly, the second term in (28) can be evaluated. So (28) is

$$\begin{aligned} & \mathbb{E} \left[\Psi^{-1} \left(\frac{R_i}{N+1} \right) \cdot \mathbf{1}(\text{sgn}(T_i) \cdot X_i(1) < 0) \right] \\ &= \frac{1}{2} \int_{\mathcal{R}_1} u(y) q^+(y) dy + \frac{1}{2} \int_{\mathcal{R}_2} u(y) q^-(y) dy, \end{aligned} \quad (32)$$

which does not depend upon the index i , and consequently, (27) becomes

$$\mathbb{E}[D(1)] = \frac{1}{2} \int_{\mathcal{R}_1} u(y) q^+(y) dy + \frac{1}{2} \int_{\mathcal{R}_2} u(y) q^-(y) dy. \quad (33)$$

The asymptotic behavior of $u(y)$ is given by Lemma 11 in Appendix F. We thus obtain

$$\begin{aligned} \lim_{N \rightarrow \infty} \mathbb{E}[D(1)] &= \frac{1}{2} \int_{\mathcal{R}_1} \left| \ln \frac{q^+(y)}{q^-(y)} \right| q^+(y) dy \\ & \quad + \frac{1}{2} \int_{\mathcal{R}_2} \left| \ln \frac{q^+(y)}{q^-(y)} \right| q^-(y) dy. \end{aligned} \quad (34)$$

APPENDIX B PROOFS OF LEMMAS 2, 5, AND 8

These three lemmas indicate that the variance of the decoding metric under $w = 1$ asymptotically vanish as $N \rightarrow \infty$. Due to their similarity, we only provide the proof of Lemma 2. Lemmas 5 and 8 appear in the proofs of Theorems 2 and 3, respectively, in Appendix E.

$$\begin{aligned}
\mathbb{E}[W_i W_j] &= \mathbb{E} \left[\Psi^{-1} \left(\frac{R_i}{N+1} \right) \Psi^{-1} \left(\frac{R_j}{N+1} \right) \cdot \mathbf{1}(\text{sgn}(T_i) \cdot X_i(1) < 0) \mathbf{1}(\text{sgn}(T_j) \cdot X_j(1) < 0) \right] \\
&= \frac{1}{4} \mathbb{E} \left[\Psi^{-1} \left(\frac{R_i}{N+1} \right) \Psi^{-1} \left(\frac{R_j}{N+1} \right) \cdot \mathbf{1}(T_i < 0) \mathbf{1}(T_j < 0) \middle| X_i(1) = +1, X_j(1) = +1 \right] \\
&\quad + \frac{1}{4} \mathbb{E} \left[\Psi^{-1} \left(\frac{R_i}{N+1} \right) \Psi^{-1} \left(\frac{R_j}{N+1} \right) \cdot \mathbf{1}(T_i > 0) \mathbf{1}(T_j < 0) \middle| X_i(1) = -1, X_j(1) = +1 \right] \\
&\quad + \frac{1}{4} \mathbb{E} \left[\Psi^{-1} \left(\frac{R_i}{N+1} \right) \Psi^{-1} \left(\frac{R_j}{N+1} \right) \cdot \mathbf{1}(T_i < 0) \mathbf{1}(T_j > 0) \middle| X_i(1) = +1, X_j(1) = -1 \right] \\
&\quad + \frac{1}{4} \mathbb{E} \left[\Psi^{-1} \left(\frac{R_i}{N+1} \right) \Psi^{-1} \left(\frac{R_j}{N+1} \right) \cdot \mathbf{1}(T_i > 0) \mathbf{1}(T_j > 0) \middle| X_i(1) = -1, X_j(1) = -1 \right], \tag{37}
\end{aligned}$$

$$\begin{aligned}
&\mathbb{E} \left[\Psi^{-1} \left(\frac{R_i}{N+1} \right) \Psi^{-1} \left(\frac{R_j}{N+1} \right) \cdot \mathbf{1}(T_i < 0) \mathbf{1}(T_j < 0) \middle| X_i(1) = +1, X_j(1) = +1 \right] \\
&= \mathbb{E} \left[\mathbb{E} \left[\Psi^{-1} \left(\frac{R_i}{N+1} \right) \Psi^{-1} \left(\frac{R_j}{N+1} \right) \cdot \mathbf{1}(T_i < 0) \mathbf{1}(T_j < 0) \middle| X_i(1) = +1, X_j(1) = +1, Y_i, Y_j \right] \right], \tag{38}
\end{aligned}$$

Define $W_i = \Psi^{-1} \left(\frac{R_i}{N+1} \right) \cdot \mathbf{1}(\text{sgn}(T_i) \cdot X_i(1) < 0)$ and $\tilde{W}_i = W_i - \mathbb{E}[W_i]$. Then for the decoding metric (6) of CDF-ORBGRAND, it follows that

$$\text{varD}(1) = \frac{1}{N^2} \sum_{i=1}^N \sum_{j=1}^N \mathbb{E}[\tilde{W}_i \tilde{W}_j]. \tag{35}$$

For $i = j$, we have $\mathbb{E}[\tilde{W}_i \tilde{W}_j] = \mathbb{E}[W_i^2] - \mathbb{E}[W_i]^2$, where $\lim_{N \rightarrow \infty} \mathbb{E}[W_i]$ has been obtained in (34), and following similar steps as those in the proof of Lemma 1, we obtain

$$\begin{aligned}
\lim_{N \rightarrow \infty} \mathbb{E}[W_i^2] &= \frac{1}{2} \int_{\mathcal{R}_1} \left| \ln \frac{q^+(y)}{q^-(y)} \right|^2 q^+(y) dy \\
&\quad + \frac{1}{2} \int_{\mathcal{R}_2} \left| \ln \frac{q^+(y)}{q^-(y)} \right|^2 q^-(y) dy. \tag{36}
\end{aligned}$$

Based on Lemma 10 in Appendix F, we establish that $\lim_{N \rightarrow \infty} \mathbb{E}[\tilde{W}_i^2]$ remains finite. Since $\text{varD}(1)$ contains N such terms for $i = 1, \dots, N$, normalization by N^2 in (35) ensures that their contribution diminishes at a rate of $O\left(\frac{1}{N}\right)$ as N grows without bound.

For $i \neq j$, we have $\mathbb{E}[\tilde{W}_i \tilde{W}_j] = \mathbb{E}[W_i W_j] - \mathbb{E}[W_i] \mathbb{E}[W_j]$. We now turn to the evaluation of $\mathbb{E}[W_i W_j]$, which, by definition, can be expressed as (37), shown at the top of this page. The first term in (37) leads to (38) and (39), shown at the top of this page and the next page, respectively. Note that R_i and R_j in (39) are the ranks resulting from inserting $|t_i| = \left| \ln \frac{q^+(y_i)}{q^-(y_i)} \right|$ and $|t_j| = \left| \ln \frac{q^+(y_j)}{q^-(y_j)} \right|$ into a sorted array of $N-2$ i.i.d. samples of $|T|$, and we denote by $u(y_i, y_j)$ the upper branch of (39). Therefore, (38) can be rewritten as $\int_{\mathcal{R}_1} \int_{\mathcal{R}_1} u(y_i, y_j) q^+(y_i) q^+(y_j) dy_i dy_j$. Applying a similar procedure to the other three terms in (37), we obtain

$$\begin{aligned}
\mathbb{E}[W_i W_j] &= \frac{1}{4} \int_{\mathcal{R}_1} \int_{\mathcal{R}_1} u(y_i, y_j) q^+(y_i) q^+(y_j) dy_i dy_j \\
&\quad + \frac{1}{4} \int_{\mathcal{R}_1} \int_{\mathcal{R}_2} u(y_i, y_j) q^-(y_i) q^+(y_j) dy_i dy_j \\
&\quad + \frac{1}{4} \int_{\mathcal{R}_2} \int_{\mathcal{R}_1} u(y_i, y_j) q^+(y_i) q^-(y_j) dy_i dy_j \\
&\quad + \frac{1}{4} \int_{\mathcal{R}_2} \int_{\mathcal{R}_2} u(y_i, y_j) q^-(y_i) q^-(y_j) dy_i dy_j. \tag{40}
\end{aligned}$$

By applying Lemma 12 in Appendix F, we obtain that $\lim_{N \rightarrow \infty} \mathbb{E}[\tilde{W}_i \tilde{W}_j] = 0$. Since $\text{varD}(1)$ contains $N \times (N-1)$ such terms for $i, j = 1, \dots, N$, normalization by N^2 in (35) ensures that their contribution diminishes as N grows without bound.

Summarizing the cases discussed, we see that $\text{varD}(1)$ asymptotically vanishes as $N \rightarrow \infty$.

APPENDIX C PROOFS OF LEMMAS 3, 6, AND 9

A. Proof of Lemma 3

For any $w' \neq 1$, the conditional expectation of the CDF-ORBGRAND decoding metric (6) satisfies

$$\begin{aligned}
&\mathbb{E} \left\{ e^{N\theta D(w')} \middle| \mathbf{T} \right\} \\
&= \mathbb{E} \left\{ \prod_{i=1}^N e^{\theta \Psi^{-1} \left(\frac{R_i}{N+1} \right) \cdot \mathbf{1}(\text{sgn}(T_i) \cdot X_i(w') < 0)} \middle| \mathbf{T} \right\} \\
&= \prod_{i=1}^N \mathbb{E} \left\{ e^{\theta \Psi^{-1} \left(\frac{R_i}{N+1} \right) \cdot \mathbf{1}(\text{sgn}(T_i) \cdot X_i(w') < 0)} \middle| \mathbf{T} \right\}, \tag{41}
\end{aligned}$$

$$\begin{aligned}
& \mathbb{E} \left[\Psi^{-1} \left(\frac{R_i}{N+1} \right) \Psi^{-1} \left(\frac{R_j}{N+1} \right) \cdot \mathbf{1}(\tau_i < 0) \mathbf{1}(\tau_j < 0) \middle| X_i(1) = +1, X_j(1) = +1, Y_i = y_i, Y_j = y_j \right] \\
&= \begin{cases} \mathbb{E} \left[\Psi^{-1} \left(\frac{R_i}{N+1} \right) \Psi^{-1} \left(\frac{R_j}{N+1} \right) \middle| X_i(1) = +1, X_j(1) = +1, Y_i = y_i, Y_j = y_j \right] & \text{if } q^+(y_i) < q^-(y_i), q^+(y_j) < q^-(y_j), \\ 0 & \text{else.} \end{cases}
\end{aligned} \tag{39}$$

where we use the fact that $\underline{\mathbb{T}}$ is induced by $\underline{X}(1)$ and is therefore independent of $\underline{X}(w')$. Each term in (41) is

$$\begin{aligned}
& \mathbb{E} \left\{ e^{\theta \Psi^{-1} \left(\frac{R_i}{N+1} \right) \cdot \mathbf{1}(\text{sgn}(\tau_i) \cdot X_i(w') < 0)} \middle| \underline{\mathbb{T}} \right\} \\
&= \frac{1}{2} \mathbb{E} \left\{ e^{\theta \Psi^{-1} \left(\frac{R_i}{N+1} \right) \cdot \mathbf{1}(\tau_i < 0)} \middle| \underline{\mathbb{T}}, X_i(w') = +1 \right\} \\
&\quad + \frac{1}{2} \mathbb{E} \left\{ e^{\theta \Psi^{-1} \left(\frac{R_i}{N+1} \right) \cdot \mathbf{1}(\tau_i > 0)} \middle| \underline{\mathbb{T}}, X_i(w') = -1 \right\} \\
&= \frac{1}{2} e^{\theta \Psi^{-1} \left(\frac{R_i}{N+1} \right) \cdot \mathbf{1}(\tau_i < 0)} + \frac{1}{2} e^{\theta \Psi^{-1} \left(\frac{R_i}{N+1} \right) \cdot \mathbf{1}(\tau_i > 0)} \\
&= \frac{1}{2} \left(1 + e^{\theta \Psi^{-1} \left(\frac{R_i}{N+1} \right)} \right),
\end{aligned} \tag{42}$$

where since R_i is determined by $\underline{\mathbb{T}}$, the conditional expectation can be suppressed. Therefore, we have

$$\begin{aligned}
& \frac{1}{N} \ln \mathbb{E} \left\{ e^{N\theta D(w')} \middle| \underline{\mathbb{T}} \right\} \\
&= \frac{1}{N} \sum_{i=1}^N \ln \left(1 + e^{\theta \Psi^{-1} \left(\frac{R_i}{N+1} \right)} \right) - \ln 2 \\
&= \frac{1}{N} \sum_{n=1}^N \ln \left(1 + e^{\theta \Psi^{-1} \left(\frac{n}{N+1} \right)} \right) - \ln 2,
\end{aligned} \tag{43}$$

where we use the fact that $\{R_i\}_{i=1, \dots, N}$ is a permutation of $\{1, \dots, N\}$. Thus, we obtain

$$\begin{aligned}
& \lim_{N \rightarrow \infty} \frac{1}{N} \ln \mathbb{E} \left\{ e^{N\theta D(w')} \middle| \underline{\mathbb{T}} \right\} \\
&= \lim_{N \rightarrow \infty} \frac{1}{N} \sum_{n=1}^N \ln \left(1 + e^{\theta \Psi^{-1} \left(\frac{n}{N+1} \right)} \right) - \ln 2 \\
&= \int_0^1 \ln \left(1 + e^{\theta \Psi^{-1}(u)} \right) du - \ln 2 \\
&= \int_0^\infty \ln \left(1 + e^{\theta t} \right) \Psi'(t) dt - \ln 2 \\
&= \mathbb{E} \left[\ln \left(1 + e^{\theta \cdot \left| \ln \frac{q^+(Y)}{q^-(Y)} \right|} \right) \right] - \ln 2,
\end{aligned} \tag{44}$$

which completes the proof.

B. Proof of Lemma 6

By following similar steps in the proof of Lemma 3, for any $w' \neq 1$, the conditional expectation of the CDF-ORBGRAND

decoding metric for BICM in (53) satisfies

$$\begin{aligned}
& \frac{1}{N} \ln \mathbb{E} \left\{ e^{N\theta D(w')} \middle| \underline{\mathbb{T}} \right\} \\
&= \frac{1}{N} \sum_{i=1}^N \sum_{j=1}^m \ln \left(1 + e^{\frac{\theta}{m} \bar{\Psi}^{-1} \left(\frac{R_{i,j}}{mN+1} \right)} \right) - m \ln 2 \\
&= \frac{1}{N} \sum_{n=1}^{mN} \ln \left(1 + e^{\frac{\theta}{m} \bar{\Psi}^{-1} \left(\frac{n}{mN+1} \right)} \right) - m \ln 2.
\end{aligned} \tag{45}$$

Thus, we obtain

$$\begin{aligned}
& \lim_{N \rightarrow \infty} \frac{1}{N} \ln \mathbb{E} \left\{ e^{N\theta D(w')} \middle| \underline{\mathbb{T}} \right\} \\
&= m \int_0^1 \ln \left(1 + e^{\frac{\theta}{m} \bar{\Psi}^{-1}(u)} \right) du - m \ln 2 \\
&= m \int_0^\infty \ln \left(1 + e^{\frac{\theta}{m} t} \right) \bar{\Psi}'(t) dt - m \ln 2 \\
&= m \int_0^\infty \ln \left(1 + e^{\frac{\theta}{m} t} \right) \cdot \left(\frac{1}{m} \sum_{j=1}^m \Psi'_j(t) \right) dt - m \ln 2 \\
&= \sum_{j=1}^m \int_0^\infty \ln \left(1 + e^{\frac{\theta}{m} t} \right) \Psi'_j(t) dt - m \ln 2 \\
&= \sum_{j=1}^m \mathbb{E} \left[\ln \left(1 + e^{\frac{\theta}{m} \cdot \left| \ln \frac{q_j^+(Y)}{q_j^-(Y)} \right|} \right) \right] - m \ln 2,
\end{aligned} \tag{46}$$

which completes the proof.

C. Proof of Lemma 9

By following similar steps in the proof of Lemma 3, for any $w' \neq 1$, the conditional expectation of the ORBGRAND decoding metric for BICM in (60) satisfies

$$\begin{aligned}
\frac{1}{N} \ln \mathbb{E} \left\{ e^{N\theta D(w')} \middle| \underline{\mathbb{T}} \right\} &= \frac{1}{N} \sum_{n=1}^{mN} \ln \left(1 + e^{\frac{\theta}{m} \cdot \frac{n}{mN}} \right) - m \ln 2 \\
&\rightarrow m \int_0^1 \ln \left(1 + e^{\frac{\theta}{m} t} \right) dt - m \ln 2
\end{aligned} \tag{47}$$

as $N \rightarrow \infty$, which completes the proof.

APPENDIX D

EQUIVALENCE OF BICM DECODER (23) AND SGRAND

The decoding rule of SGRAND for BICM can be equivalently expressed as

$$\hat{w} = \arg \min_{w=1, \dots, \lceil e^{NR} \rceil} \sum_{i=1}^N \sum_{j=1}^m \left| \ln \frac{q_j^+(y_i)}{q_j^-(y_i)} \right| \cdot \mathbf{1} \left(\operatorname{sgn} \left(\ln \frac{q_j^+(y_i)}{q_j^-(y_i)} \right) \cdot x_{i,j}(w) < 0 \right). \quad (48)$$

Likewise, the BICM decoding rule (23) can be equivalently expressed by

$$\hat{w} = \arg \max_{w=1, \dots, \lceil e^{NR} \rceil} \sum_{i=1}^N \sum_{j=1}^m \ln d_j(b_j(s_i(w)), y_i), \quad (49)$$

where $d_j(+1, y) = q_j^+(y)$ and $d_j(-1, y) = q_j^-(y)$.

The summation in (48) can be expanded as

$$\begin{aligned} & \sum_{(i,j): x_{i,j}(w)=+1, q_j^+(y_i) < q_j^-(y_i)} [\ln q_j^-(y_i) - \ln q_j^+(y_i)] \\ + & \sum_{(i,j): x_{i,j}(w)=-1, q_j^+(y_i) > q_j^-(y_i)} [\ln q_j^+(y_i) - \ln q_j^-(y_i)], \quad (50) \end{aligned}$$

and the summation in (49) is

$$\sum_{(i,j): x_{i,j}(w)=+1} \ln q_j^+(y_i) + \sum_{(i,j): x_{i,j}(w)=-1} \ln q_j^-(y_i). \quad (51)$$

The sum of (50) and (51), after simplification, turns out to be a constant

$$\sum_{i=1}^N \sum_{j=1}^m \max \{ \ln q_j^+(y_i), \ln q_j^-(y_i) \}. \quad (52)$$

Therefore, the two decoding rules are equivalent.

APPENDIX E

PROOFS OF THEOREMS 2 AND 3

A. Proof of Theorem 2

Based on the unified decoding rule (24), the decoding metric of CDF-ORBGRAND for BICM is given by

$$\begin{aligned} D(w) &= \frac{1}{mN} \sum_{i=1}^N \sum_{j=1}^m \bar{\Psi}^{-1} \left(\frac{R_{i,j}}{mN+1} \right) \\ & \quad \mathbf{1} (\operatorname{sgn} (\mathbb{T}_{i,j}) \cdot X_{i,j}(w) < 0), \quad w = 1, \dots, \lceil e^{NR} \rceil. \quad (53) \end{aligned}$$

Under the condition that the transmitted message is $w = 1$, the following lemmas characterize some asymptotic properties of the CDF-ORBGRAND decoding metric (53). The proofs of these lemmas are provided in the preceding appendices.

Lemma 4: As $N \rightarrow \infty$, the expected value of the decoding metric (53) for the transmitted codeword is given by

$$\begin{aligned} \lim_{N \rightarrow \infty} \mathbb{E} D(1) &= \frac{1}{m} \sum_{j=1}^m \left(\frac{1}{2} \int_{\mathcal{R}_{1,j}} \left| \ln \frac{q_j^+(y)}{q_j^-(y)} \right| q_j^+(y) dy \right. \\ & \quad \left. + \frac{1}{2} \int_{\mathcal{R}_{2,j}} \left| \ln \frac{q_j^+(y)}{q_j^-(y)} \right| q_j^-(y) dy \right). \quad (54) \end{aligned}$$

Lemma 5: As $N \rightarrow \infty$, the variance of the decoding metric (53) for the transmitted codeword satisfies

$$\lim_{N \rightarrow \infty} \operatorname{var} D(1) = 0. \quad (55)$$

Lemma 6: As $N \rightarrow \infty$, for any non-transmitted codeword, i.e., $w' \neq 1$, and for any $\theta < 0$, the decoding metric (53) behaves almost surely as

$$\begin{aligned} & \lim_{N \rightarrow \infty} \frac{1}{N} \ln \mathbb{E} \left\{ e^{N\theta D(w')} \middle| \mathbb{T} \right\} \\ &= \sum_{j=1}^m \mathbb{E} \left[\ln \left(1 + e^{\frac{\theta}{m} \left| \ln \frac{q_j^+(Y)}{q_j^-(Y)} \right|} \right) \right] - m \ln 2. \quad (56) \end{aligned}$$

Similar to the proof of Theorem 1, we first define the event \mathcal{U}_ϵ that the decoding metric (53) for the transmitted codeword exceeds its asymptotic mean by at least ϵ . This allows us to upper bound the ensemble average error probability of decoding by $\Pr[\mathcal{U}_\epsilon] + \Pr[\hat{w} \neq 1, \mathcal{U}_\epsilon^c]$. Using Lemmas 4 and 5 together with Chebyshev inequality, we obtain that $\Pr[\mathcal{U}_\epsilon] \rightarrow 0$ as $N \rightarrow \infty$. On the other hand, by applying Lemma 6, we deduce that for any R satisfying

$$\begin{aligned} R &< I_{\text{CDF-ORB,BICM}} := m \ln 2 \\ & - \inf_{\theta < 0} \left\{ \sum_{j=1}^m \left(\mathbb{E} \left[\ln \left(1 + e^{\frac{\theta}{m} \left| \ln \frac{q_j^+(Y)}{q_j^-(Y)} \right|} \right) \right] \right. \right. \\ & - \frac{\theta}{m} \cdot \frac{1}{2} \int_{\mathcal{R}_{1,j}} \left| \ln \frac{q_j^+(y)}{q_j^-(y)} \right| q_j^+(y) dy \\ & \left. \left. - \frac{\theta}{m} \cdot \frac{1}{2} \int_{\mathcal{R}_{2,j}} \left| \ln \frac{q_j^+(y)}{q_j^-(y)} \right| q_j^-(y) dy \right) \right\} \quad (57) \end{aligned}$$

in nats/channel use, the average error probability of decoding asymptotically vanishes as $N \rightarrow \infty$.

By setting $\eta = \frac{\theta}{m}$, the right side of (57) can be written as

$$\begin{aligned} & \sup_{\eta < 0} \left\{ \sum_{j=1}^m \left(\ln 2 - \mathbb{E} \left[\ln \left(1 + e^{\eta \left| \ln \frac{q_j^+(Y)}{q_j^-(Y)} \right|} \right) \right] \right. \right. \\ & \left. \left. + \frac{\eta}{2} \int_{\mathcal{R}_{1,j}} \left| \ln \frac{q_j^+(y)}{q_j^-(y)} \right| q_j^+(y) dy + \frac{\eta}{2} \int_{\mathcal{R}_{2,j}} \left| \ln \frac{q_j^+(y)}{q_j^-(y)} \right| q_j^-(y) dy \right) \right\} \\ &= \sup_{\eta < 0} \left\{ \sum_{j=1}^m f_j(\eta) \right\}. \quad (58) \end{aligned}$$

From the proof of Theorem 1 in Section III-B, we know that for each $j = 1, \dots, m$, $f_j(\eta)$ attains its extreme at $\eta = -1$ and $f_j(-1) = I(X_j; Y)$. Hence, we have the achievable rate of CDF-ORBGRAND for BICM

$$I_{\text{CDF-ORB,BICM}} = \sup_{\eta < 0} \left\{ \sum_{j=1}^m f_j(\eta) \right\} = \sum_{j=1}^m I(X_j; Y) = C^{\text{BICM}}, \quad (59)$$

thereby completing the proof.

B. Proof of Theorem 3

Based on the unified decoding rule (24), the decoding metric of ORBGRAND for BICM is given by

$$D(w) = \frac{1}{mN} \sum_{i=1}^N \sum_{j=1}^m \frac{R_{i,j}}{mN} \cdot \mathbf{1}(\text{sgn}(\mathbb{T}_{i,j}) \cdot X_{i,j}(w) < 0), w = 1, \dots, \lceil e^{NR} \rceil. \quad (60)$$

Under the condition that the transmitted message is $w = 1$, the following lemmas characterize some asymptotic properties of the ORBGRAND decoding metric (60). The proofs of these lemmas are provided in the preceding appendices.

Lemma 7: As $N \rightarrow \infty$, the expected value of the decoding metric (60) for the transmitted codeword is given by

$$\lim_{N \rightarrow \infty} \mathbb{E}D(1) = \frac{1}{m} \sum_{j=1}^m \left(\frac{1}{2} \int_{\mathcal{R}_{1,j}} \bar{\Psi} \left(\left| \ln \frac{q_j^+(y)}{q_j^-(y)} \right| \right) q_j^+(y) dy + \frac{1}{2} \int_{\mathcal{R}_{2,j}} \bar{\Psi} \left(\left| \ln \frac{q_j^+(y)}{q_j^-(y)} \right| \right) q_j^-(y) dy \right). \quad (61)$$

Lemma 8: As $N \rightarrow \infty$, the variance of the decoding metric (60) for the transmitted codeword satisfies

$$\lim_{N \rightarrow \infty} \text{var}D(1) = 0. \quad (62)$$

Lemma 9: As $N \rightarrow \infty$, for any non-transmitted codeword, i.e., $w' \neq 1$, and for any $\theta < 0$, the decoding metric (60) behaves almost surely as

$$\lim_{N \rightarrow \infty} \frac{1}{N} \ln \mathbb{E} \left\{ e^{N\theta D(w')} \middle| \mathbb{T} \right\} = m \int_0^1 \ln(1 + e^{\frac{\theta}{m}t}) dt - m \ln 2. \quad (63)$$

Based on these lemmas, we can complete the proof of Theorem 3 following steps similar to those used in the proofs of Theorems 1 and 2.

As a side remark, we compare $I_{\text{ORB,BICM}}$ with the achievable rate derived in our previous work [25], where we assumed ideal interleaving (see Fig. 2) and hence the achievable rate is simply the sum of GMIs over the m bit channels, i.e.,

$$\begin{aligned} \tilde{I}_{\text{ORB,BICM}} &= \sum_{j=1}^m I_{\text{ORB},j} \\ &= m \ln 2 - \sum_{j=1}^m \inf_{\theta_j < 0} \left\{ \int_0^1 \ln(1 + e^{\theta_j t}) dt \right. \\ &\quad \left. - \theta_j \cdot \frac{1}{2} \int_{\mathcal{R}_{1,j}} \Psi_j \left(\left| \ln \frac{q_j^+(y)}{q_j^-(y)} \right| \right) q_j^+(y) dy \right. \\ &\quad \left. - \theta_j \cdot \frac{1}{2} \int_{\mathcal{R}_{2,j}} \Psi_j \left(\left| \ln \frac{q_j^+(y)}{q_j^-(y)} \right| \right) q_j^-(y) dy \right\}. \quad (64) \end{aligned}$$

In contrast to $I_{\text{ORB,BICM}}$ given by (26), here the expression (64) suggests that coding is done separately over different bit channels, rather than across them jointly. When all bit channels have identical laws, i.e., $q_j^\pm(y)$ being the same for $j = 1, \dots, m$, $I_{\text{ORB,BICM}}$ and $\tilde{I}_{\text{ORB,BICM}}$ coincide. Nevertheless, as shown in our numerical results in Section IV-E, their discrepancy is typically negligible.

APPENDIX F SUPPORTING LEMMAS

Lemma 10: If $q^+(y)$ and $q^-(y)$ satisfy Assumptions 1 and 2, then

$$\begin{aligned} &\frac{1}{2} \int_{\mathcal{R}_1} \left| \ln \frac{q^+(y)}{q^-(y)} \right|^2 q^+(y) dy + \frac{1}{2} \int_{\mathcal{R}_2} \left| \ln \frac{q^+(y)}{q^-(y)} \right|^2 q^-(y) dy \\ &- \left(\frac{1}{2} \int_{\mathcal{R}_1} \left| \ln \frac{q^+(y)}{q^-(y)} \right| q^+(y) dy + \frac{1}{2} \int_{\mathcal{R}_2} \left| \ln \frac{q^+(y)}{q^-(y)} \right| q^-(y) dy \right)^2 \end{aligned} \quad (65)$$

is a finite value.

Proof: Considering the first term in (65), there exists a sufficiently large constant M such that

$$\begin{aligned} &\int_{\mathcal{R}_1} \left| \ln \frac{q^+(y)}{q^-(y)} \right|^2 q^+(y) dy \\ &\leq \int_{|y| < M} \left| \ln \frac{q^+(y)}{q^-(y)} \right|^2 q^+(y) dy + \int_{|y| \geq M} \left| \ln \frac{q^+(y)}{q^-(y)} \right|^2 q^+(y) dy \\ &\leq \int_{|y| < M} \left| \ln \frac{q^+(y)}{q^-(y)} \right|^2 q^+(y) dy + \int_{|y| \geq M} S_2^2(|y|) S_1(|y|) e^{-a|y|} dy. \end{aligned} \quad (66)$$

The first term of (67) is the integral of a bounded function over a bounded interval, so it is finite; the second term of (67) is also finite, as light-tailed distributions admit all moments. Therefore, (66) is bounded. Applying analogous argument to the other three terms in (65) shows that all the integrals involved are finite, and hence (65) is finite. ■

Lemma 11: Suppose that the CDFs of $|\mathbb{T}_{\cdot,1}|, \dots, |\mathbb{T}_{\cdot,m}|$ all satisfy Assumption 3. Denote by $R(v)$ the rank of v when inserted into the sorted array consisting of independent samples $\{|\mathbb{T}_{1,1}|, \dots, |\mathbb{T}_{1,m}|, \dots, |\mathbb{T}_{N,1}|, \dots, |\mathbb{T}_{N,m}|\}$, with an arbitrary one of them removed. We have

$$\lim_{N \rightarrow \infty} \frac{\mathbb{E}[R(v)]}{mN} = \bar{\Psi}(v), \quad (68)$$

$$\lim_{N \rightarrow \infty} \frac{\mathbb{E}[R(v)^2]}{m^2 N^2} = \bar{\Psi}(v)^2, \quad (69)$$

$$\lim_{N \rightarrow \infty} \mathbb{E} \left[\bar{\Psi}^{-1} \left(\frac{R(v)}{mN+1} \right) \right] = v, \quad (70)$$

$$\lim_{N \rightarrow \infty} \mathbb{E} \left[\left(\bar{\Psi}^{-1} \left(\frac{R(v)}{mN+1} \right) \right)^2 \right] = v^2. \quad (71)$$

Proof: Without loss of generality, we remove $|\mathbb{T}_{N,m}|$, and the proof holds with very minor modification if we remove any other sample.

Based on the definition of $R(v)$, we have

$$R(v) = 1 + \sum_{i=1}^{N-1} \sum_{j=1}^m \mathbf{1}(|\mathbb{T}_{i,j}| < v) + \sum_{j=1}^{m-1} \mathbf{1}(|\mathbb{T}_{N,j}| < v). \quad (72)$$

Taking the expectation of (72) yields

$$\mathbb{E}[R(v)] = 1 + (N-1) \sum_{j=1}^m \Psi_j(v) + \sum_{j=1}^{m-1} \Psi_j(v), \quad (73)$$

from which (68) immediately follows. Taking the expectation of the square of (72) and conducting a few algebraic manipulation steps yield (69).

Denoting $G(\cdot) = \bar{\Psi}^{-1}(\cdot)$, $S = \frac{R(v)}{mN+1}$ and $p = \bar{\Psi}(v)$, we can show that as $N \rightarrow \infty$,

$$\mathbb{E}[S - p] = O\left(\frac{1}{N}\right), \mathbb{E}[(S - p)^2] = O\left(\frac{1}{N}\right), \quad (74)$$

$$\mathbb{E}[|S - p|^3] \leq O\left(\frac{1}{N^{\frac{3}{2}}}\right). \quad (75)$$

We perform a Taylor expansion of $G(S)$ around p :

$$G(S) = G(p) + G'(p)(S - p) + \frac{1}{2}G''(p)(S - p)^2 + K_3, \quad (76)$$

where the residual term satisfies

$$|K_3| \leq \frac{1}{6} \sup_{u \in [p-\delta, p+\delta]} |G'''(u)| \cdot |S - p|^3.$$

Taking the expectation of (76), substituting (74) and (75), and applying Assumption 3, we obtain (70).

Similarly, performing a Taylor expansion of $G(S)^2$ around p and taking its expectation, we obtain (71). ■

Lemma 12: Suppose that the CDFs of $|\mathbb{T}_{\cdot,1}|, \dots, |\mathbb{T}_{\cdot,m}|$ all satisfy Assumption 3. Denote by $R(v_a)$ and $R(v_b)$ the ranks of v_a and v_b , respectively, when inserted into the sorted array consisting of independent samples $\{|\mathbb{T}_{1,1}|, \dots, |\mathbb{T}_{1,m}|, \dots, |\mathbb{T}_{N,1}|, \dots, |\mathbb{T}_{N,m}|\}$, with arbitrary two of them removed. We have

$$\lim_{N \rightarrow \infty} \frac{\mathbb{E}[R(v_a)R(v_b)]}{m^2 N^2} = \bar{\Psi}(v_a)\bar{\Psi}(v_b), \quad (77)$$

$$\lim_{N \rightarrow \infty} \mathbb{E}\left[\bar{\Psi}^{-1}\left(\frac{R(v_a)}{mN+1}\right)\bar{\Psi}^{-1}\left(\frac{R(v_b)}{mN+1}\right)\right] = v_a v_b. \quad (78)$$

Proof: Without loss of generality, we remove $|\mathbb{T}_{N,m-1}|$ and $|\mathbb{T}_{N,m}|$, and the proof holds with very minor modification if we remove any other two samples.

Based on the definition of $R(v_a)$ and $R(v_b)$, we can deduce that

$$\mathbb{E}[R(v_a)R(v_b)] = N^2 \sum_{i=1}^m \sum_{j=1}^m \Psi_i(v_a)\Psi_j(v_b) + O(N), \quad (79)$$

from which (77) immediately follows.

Denoting $G(\cdot) = \bar{\Psi}^{-1}(\cdot)$, $S_a = \frac{R(v_a)}{mN+1}$, $S_b = \frac{R(v_b)}{mN+1}$, $p_a = \bar{\Psi}(v_a)$ and $p_b = \bar{\Psi}(v_b)$, and following the similar approach for the proof of (70), we perform Taylor expansions of $G(S_a)$ and $G(S_b)$ around p_a and p_b , respectively; then multiplying these Taylor expansions and taking the expectation lead to (78). ■

REFERENCES

- [1] K. R. Duffy, J. Li, and M. Médard, "Capacity-achieving guessing random additive noise decoding," *IEEE Trans. Inf. Theory*, vol. 65, no. 7, pp. 4023–4040, 2019.
- [2] A. Riaz, M. Medard, K. R. Duffy, and R. T. Yazicigil, "A universal maximum likelihood GRAND decoder in 40nm CMOS," in *Proc. 14th Int. Conf. on Commun. Syst. NETw. (COMSNETS)*, 2022, pp. 421–423.
- [3] Q. Wang, J. Liang, P. Yuan, K. R. Duffy, M. Médard, and X. Ma, "Guessing decoding of short blocklength codes," 2025, *arxiv:2511.12108*.
- [4] S. Lin and D. J. Costello, *Error Control Coding, 2nd ed.* Pearson, 2004.
- [5] K. R. Duffy, M. Médard, and W. An, "Guessing random additive noise decoding with symbol reliability information (SRGRAND)," *IEEE Trans. Commun.*, vol. 70, no. 1, pp. 3–18, 2021.
- [6] A. Solomon, K. R. Duffy, and M. Médard, "Soft maximum likelihood decoding using GRAND," in *Proc. IEEE Int. Conf. Commun. (ICC)*, 2020, pp. 1–6.
- [7] K. R. Duffy, W. An, and M. Médard, "Ordered reliability bits guessing random additive noise decoding," *IEEE Trans. Signal Process.*, vol. 70, pp. 4528–4542, 2022.
- [8] C. Condo, V. Bioglio, and I. Land, "High-performance low-complexity error pattern generation for ORBGRAND decoding," in *Proc. IEEE Globecom Workshops*, 2021, pp. 1–6.
- [9] S. M. Abbas, T. Tonnellier, F. Ercan, M. Jaleddine, and W. J. Gross, "High-throughput and energy-efficient VLSI architecture for ordered reliability bits GRAND," *IEEE Trans. Very Large Scale Integr. (VLSI) Syst.*, vol. 30, no. 6, pp. 681–693, 2022.
- [10] C. Condo, "A fixed latency ORBGRAND decoder architecture with LUT-aided error-pattern scheduling," *IEEE Trans. Circuits Sys. I: Reg. Papers*, vol. 69, no. 5, pp. 2203–2211, 2022.
- [11] M. Liu, Y. Wei, Z. Chen, and W. Zhang, "ORBGRAND is almost capacity-achieving," *IEEE Trans. Inf. Theory*, vol. 69, no. 5, pp. 2830–2840, 2022.
- [12] H. Sarrideen, M. Médard, and K. R. Duffy, "GRAND for fading channels using pseudo-soft information," in *Proc. IEEE Global Commun. Conf. (GLOBECOM)*, 2022, pp. 3502–3507.
- [13] S. M. Abbas, M. Jaleddine, and W. J. Gross, "GRAND for Rayleigh fading channels," in *Proc. IEEE Globecom Workshops*, 2022, pp. 504–509.
- [14] S. M. Abbas, M. Jaleddine, and W. J. Gross, "Hardware architecture for fading-GRAND," in *Guessing Random Additive Noise Decoding: A Hardware Perspective*. Springer, 2023, pp. 125–140.
- [15] I. Chatzigeorgiou and F. A. Monteiro, "Symbol-level GRAND for high-order modulation over block fading channels," *IEEE Commun. Lett.*, vol. 27, no. 2, pp. 447–451, 2022.
- [16] S. Allahkaram, F. A. Monteiro, and I. Chatzigeorgiou, "URLLC with coded massive MIMO via random linear codes and GRAND," in *Proc. IEEE 96th Veh. Technol. Conf. (VTC-Fall)*, 2022, pp. 1–5.
- [17] S. Allahkaram, F. A. Monteiro, and I. Chatzigeorgiou, "Symbol-level noise-guessing decoding with antenna sorting for URLLC massive MIMO," 2023, *arXiv:2305.13113*.
- [18] L. Wan and W. Zhang, "Approaching maximum likelihood decoding performance via reshuffling ORBGRAND," in *Proc. IEEE Int. Symp. Inf. Theory (ISIT)*, 2024, pp. 31–36.
- [19] L. Wan, H. Yin, and W. Zhang, "Fine-tuning ORBGRAND with very few channel soft values," in *Proc. IEEE/CIC Int. Conf. Commun. in China (ICCC Workshops)*, 2025, pp. 1–6.
- [20] G. Caire, G. Taricco, and E. Biglieri, "Bit-interleaved coded modulation," *IEEE Trans. Inf. Theory*, vol. 44, no. 3, pp. 927–946, 1998.
- [21] A. G. i Fabregas, A. Martinez, and G. Caire, "Bit-interleaved coded modulation," *Found. Trends® Commun. Inf. Theory*, vol. 5, no. 1–2, pp. 1–153, 2008.
- [22] A. Martinez, A. G. i Fabregas, G. Caire, and F. M. Willems, "Bit-interleaved coded modulation revisited: A mismatched decoding perspective," *IEEE Trans. Inf. Theory*, vol. 55, no. 6, pp. 2756–2765, 2009.
- [23] A. Ganti, A. Lapidoth, and I. E. Telatar, "Mismatched decoding revisited: General alphabets, channels with memory, and the wide-band limit," *IEEE Trans. Inf. Theory*, vol. 46, no. 7, pp. 2315–2328, 2000.
- [24] A. Lapidoth and S. Shamai, "Fading channels: how perfect need 'perfect side information' be?" *IEEE Trans. Inf. Theory*, vol. 48, no. 5, pp. 1118–1134, 2002.
- [25] Z. Li and W. Zhang, "ORBGRAND: Achievable rate for general bit channels and application in BICM," in *Proc. IEEE Int. Symp. Pers., Ind., Mobile Radio Commun.*, 2024, pp. 1–7.
- [26] H. Weingarten, Y. Steinberg, and S. Shamai (Shitz), "Gaussian codes and weighted nearest neighbor decoding in fading multiple-antenna channels," *IEEE Trans. Inf. Theory*, vol. 50, no. 8, pp. 1665–1686, 2004.
- [27] E. Zehavi, "8-PSK trellis codes for a Rayleigh channel," *IEEE Trans. Commun.*, vol. 40, no. 5, pp. 873–884, 1992.